Piotr Białas, Jakub Kowal, Adam Strzelecki*, Tomasz Bednarski, Eryk Czerwiński, Krzysztof Giergiel, Łukasz Kapłon, Andrzej Kochanowski, Grzegorz Korcyl, Paweł Kowalski, Tomasz Kozik, Wojciech Krzemień, Marcin Molenda, Ines Moskal, Paweł Moskal, Szymon Niedźwiecki, Marek Pałka, Monika Pawlik, Lech Raczyński, Zbigniew Rudy, Piotr Salabura, Neha G. Sharma, Michał Silarski, Artur Słomski, Jerzy Smyrski, Konrad Szymański, Wojciech Wiślicki, Piotr Witkowski, Marcin Zieliński and Natalia Zoń

List-mode reconstruction in 2D strip PET

Abstract: Using a theory of list-mode maximum likelihood expectation-maximization (MLEM) algorithm, in this contribution, we present a derivation of the system response kernel for a novel positron emission tomography (PET) detector based on plastic scintillators.

Keywords: image reconstruction; MLEM; Monte Carlo simulation.

***Corresponding author: Adam Strzelecki,** Faculty of Physics, Astronomy and Applied Computer Science, Jagiellonian University, Reymonta 4, Room 05A, 30-059 Cracow, Poland, E-mail: adam.strzelecki@uj.edu.pl

Piotr Białas, Jakub Kowal, Adam Strzelecki, Tomasz Bednarski, Eryk Czerwiński, Krzysztof Giergiel, Grzegorz Korcyl, Tomasz Kozik, Wojciech Krzemień, Ines Moskal, Paweł Moskal, Szymon Niedźwiecki, Marek Pałka, Monika Pawlik, Zbigniew Rudy, Piotr Salabura, Neha G. Sharma, Michał Silarski, Artur Słomski, Jerzy Smyrski, Konrad Szymański, Piotr Witkowski, Marcin Zieliński and Natalia Zoń: Institute of Physics, Jagiellonian University, 30-059 Cracow, Poland

Łukasz Kapłon: Institute of Physics, Jagiellonian University, 30-059 Cracow, Poland; and Faculty of Chemistry, Jagiellonian University, 30-060 Cracow, Poland

Andrzej Kochanowski and Marcin Molenda: Faculty of Chemistry, Jagiellonian University, 30-060 Cracow, Poland

Paweł Kowalski, Lech Raczyński and Wojciech Wiślicki: Świerk Computing Centre, National Centre for Nuclear Research, 05-400 Otwock-Świerk, Poland

Introduction

The main problem in computed tomography is object reconstruction based on source emission. This is done using a set of independent events detected by positron emission tomography (PET) detectors. The PET is based on detection of the pairs of γ quanta emitted from the β^+ sources. Detecting the pair of γ quants yields a "tube of response" passing through the emission point. The better the spatial resolution of the detection, the thinner is the tube giving a better reconstruction. Achieving sufficient time resolution (<100 ps) is the main technological challenge; however, the novel hardware requires also a suitable adaptation of the reconstruction algorithm. In this paper, we are presenting a calculation of the system kernel for maximum likelihood expectation-maximization (MLEM) 2D reconstruction algorithm [1, 2] in PET prototype using the long plastic scintillators, where position is obtained from the time-of-flight measurement [3–5].

Detector geometry

For the time being, we focus on 2D detector geometry described by a two parallel line segments of scintillators of length L at the distance $2R$, with neglected thickness (Figure 1). To measure time, photomultiplier tubes are attached to each end of both scintillators. This is a minimal configuration required to form single detector and perform reconstruction.

Hit position in our geometry can be estimated by two quantities, where $c_{sci.}$ is the effective speed of light in scintillator:

$$\widetilde{z_u}=\frac{1}{2}c_{sci.}(\tilde{T}_{ul}-\tilde{T}_{ur}),\quad \widetilde{z_d}=\frac{1}{2}c_{sci.}(\tilde{T}_{dl}-\tilde{T}_{dr}) \tag{1}$$

Combining time measurements from two scintillators, we can estimate the position of the emission point on the line joining upper and lower crossing points

$$\widetilde{\Delta l}=\frac{1}{2}c((\tilde{T}_{ul}+\tilde{T}_{ur})-(\tilde{T}_{dl}+\tilde{T}_{dr})) \tag{2}$$

where Δl is the difference of distances of the reconstructed point (y,z) from upper and lower detection points.

Those quantities are, of course, subject to measurement errors and are related to exact ones by

$$\tilde{z}_y=z_y+\varepsilon_{z_y}, y=u,d \qquad \widetilde{\Delta l}=\Delta l+\varepsilon_{\Delta l}. \tag{3}$$

where the errors ε are normally distributed with correlation matrix C. In our case, the magnitude of the errors will

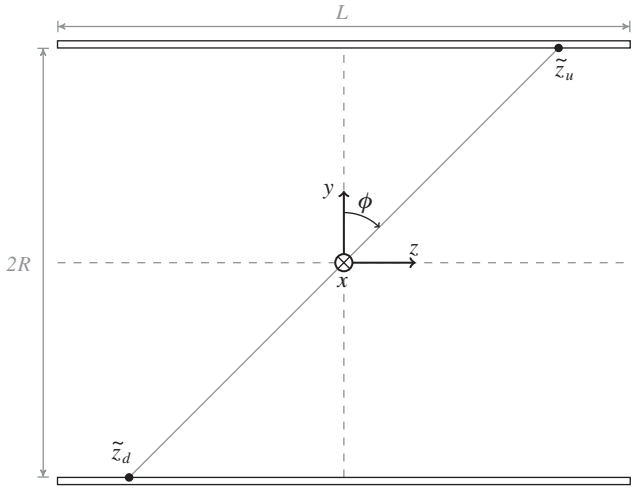

Figure 1 Detector geometry.

depend on place where the γ hit the scintillator $C=C(z_u,z_d)$. This matrix is a necessary and important input used for the reconstruction algorithm.

$$C=\begin{pmatrix}\sigma_z^2(z_u) & 0 & \gamma(z_u)\\ 0 & \sigma_z^2(z_d) & -\gamma(z_d)\\ \gamma(z_u) & -\gamma(z_d) & \sigma_{\Delta l}^2(z_u,z_d)\end{pmatrix} \tag{4}$$

where

$$\sigma_z^2(z)=\langle\varepsilon_{u(d)}^2(z)\rangle,\qquad \sigma_{\Delta l}^2(z_u,z_d)=\langle\varepsilon_{\Delta l}^2(z_u,z_d)\rangle \tag{5}$$

and

$$\gamma(z)=\langle\varepsilon_{z_u}(z)\varepsilon_{\Delta l}(z,z_d)\rangle=-\langle\varepsilon_{z_d}(z)\varepsilon_{\Delta l}(z_u,z)\rangle \tag{6}$$

List-mode reconstruction

Here we provide a very brief introduction to MLEM algorithm; for details, refer to [6].

Let $P(\tilde{\mathbf{e}}|i)$ be the system response kernel defined as probability that a detected event emitted from pixel i was reconstructed as $\tilde{\mathbf{e}}$. Using this probability for each emitter density ρ, we can compute the probability of observing the particular set of N events [7]:

$$P(\{\tilde{\mathbf{e}}_1,\ldots,\tilde{\mathbf{e}}_N\}|\rho)=\prod_j\sum_i P(\tilde{\mathbf{e}}_j|i)\frac{\rho(i)s(i)}{\sum_i\rho(i)s(i)} \tag{7}$$

The $s(i)$ is the sensitivity of the pixel; for example, the probability that an event emitted from pixel i will be detected at all.

$$s(y,z)=\pi^{-1}\int_{-\frac{\pi}{2}}^{\frac{\pi}{2}}\mathrm{d}\theta s(y,z,\theta)=\pi^{-1}(\theta_{\max}-\theta_{\min}) \tag{8}$$

with

$$\begin{aligned}\theta_{\min}&=\arctan\max\left(-\frac{\frac{1}{2}L+z}{R-y},\frac{-\frac{1}{2}L+z}{R+y}\right),\\ \theta_{\max}&=\arctan\min\left(\frac{\frac{1}{2}L-z}{R-y},\frac{\frac{1}{2}L+z}{R+y}\right).\end{aligned} \tag{9}$$

The reconstruction algorithm consists of finding the distribution ρ that maximizes this probability. That is achieved using the iterative expectation maximization (EM) algorithm [6]

$$\rho(l)^{(t+1)}=\sum_{j=1}^{N}\frac{P(\tilde{\mathbf{e}}_j|l)\rho(l)^t}{\sum_{i=1}^{M}P(\tilde{\mathbf{e}}_j|i)s(i)\rho(i)^t}. \tag{10}$$

The sum over j runs over all collected events $\{\tilde{\mathbf{e}}_j\}$. Considering that up to 100 millions of events can be collected during a single scan, this is a very time-consuming calculation, but it can be easily parallelized on current architectures.

System response kernel

We are approximating $P(\tilde{\mathbf{e}}|i)$ by system response kernel formula defined as

$$\begin{aligned}p(\tilde{\mathbf{e}}|y,z)\approx&\frac{\det{}^{\frac{1}{2}}C}{2\pi\sqrt{\vec{a}C^{-1}\vec{a}+2\vec{o}C^{-1}\vec{b}}}\pi^{-1}s(y,z)\\ &\exp\left(-\frac{1}{2}\left(\vec{b}C^{-1}\vec{b}-\frac{(\vec{b}C^{-1}\vec{a})^2}{\vec{a}C^{-1}\vec{a}+2\vec{o}C^{-1}\vec{b}}\right)\right).\end{aligned} \tag{11}$$

where

$$\vec{o}=\begin{pmatrix}-(\Delta y+\tilde{y}-R)\tan\tilde{\theta}\cos^{-2}\tilde{\theta}\\ -(\Delta y+\tilde{y}+R)\tan\tilde{\theta}\cos^{-2}\tilde{\theta}\\ -(\Delta y+\tilde{y})\cos^{-1}\tilde{\theta}(1+2\tan^2\tilde{\theta})\end{pmatrix}, \tag{12}$$

$$\vec{a}=\begin{pmatrix}-(\Delta y+\tilde{y}-R)\cos^{-2}\tilde{\theta}\\ -(\Delta y+\tilde{y}+R)\cos^{-2}\tilde{\theta}\\ -(\Delta y+\tilde{y})\cos^{-1}\tilde{\theta}\tan\tilde{\theta}\end{pmatrix} \tag{13}$$

and

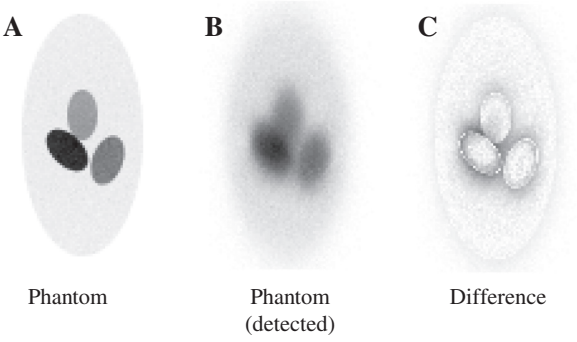

Figure 2 Phantom image versus image detected by PET and their difference.

$$\vec{b}=\begin{pmatrix}\Delta z-\Delta y\tan\tilde{\theta}\\ \Delta z-\Delta y\tan\tilde{\theta}\\ -2\Delta y\cos^{-1}\tilde{\theta}\end{pmatrix} \tag{14}$$

$$\Delta y=y-\tilde{y} \quad \text{and} \quad \Delta z=z-\tilde{z}. \tag{15}$$

After performing the integration over the pixel, we have obtained the final formula:

$$p(\tilde{\mathbf{e}}|i)\approx V(i)\,p(\tilde{\mathbf{e}}|y_i,z_i), \quad \text{and} \quad s(i)\approx V(i)s(y_i,z_i) \tag{16}$$

and

$$P(\tilde{\mathbf{e}}|i)\approx\frac{p(\tilde{\mathbf{e}}|y_i,z_i)}{s(y_i,z_i)} \tag{17}$$

where (y_i,z_i) denotes the center of pixel i.

For each event, we are calculating formula (11) that is nonzero only in a limited region around the reconstruction point. We are estimating this region by the quadratic form ellipse equation given by

$$\vec{b}C^{-1}\vec{b}=R^2 \tag{18}$$

where R is defined as the three sigma (R=3).

Simulation

Presented 2D model makes a foundation not only for final reconstruction algorithm. In order to build prototype PET detector, we need to determine initial geometry parameters that will provide good reconstruction quality. Since there are several points of freedom such as scintillator strip width, shape, and distance between scintillators, settings of detector electronics, we would not have enough time and funds to build so many prototypes representing them. Instead, this will try to determine best configuration using Monte Carlo simulation of virtual phantom inside virtual PET detector.

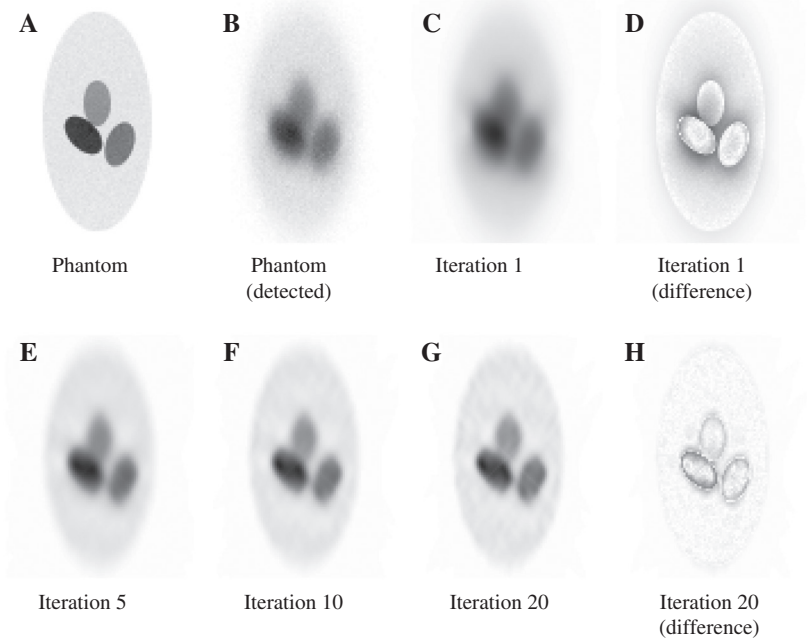

Figure 3 Reconstruction of 10^8 simulated events in 100×100-pixel image space inside 1×1 m event space (10 mm pixel size) using presented model.
Time measurement error distribution parameters were determined in our lab by controlled exposition of rectangular scintillator strip to quanta ray emitted by point source (collimator) [4].

In both cases (Monte Carlo simulation and real measurements), quality estimation will be performed comparing the perfect phantom image to the reconstructed image. We will be measuring resolution and noise – factors that have an impact on readability of the image presented to medical staff.

It is important to remark that reconstruction input is what has been detected by PET detector (Figure 2B). One can observe that there is noticeable difference between phantom (Figure 2A) and its detected image.

The difference (Figures 2C and 3D, 3H) comes from two factors: (1) a noise caused by finite number of γ quanta emitted by source and (2) a blur caused by PET detector geometry and electronics accuracy. This cannot be avoided; moreover, reducing one factor can raise the other, such that reducing scintillator diameter improves resolution but reduces acceptance, causing more noise. Therefore, the goal is to find perfect balance.

Obviously, our model is rough approximation, possibly to simulate using available computer power and accurate enough to get initial hints on how to build the first prototypes. Once such prototype is built, we can proceed with real measurements done on physical phantom to reevaluate reconstruction quality and our model approximation as well.

Summary

We have presented a 2D strip scintillator PET model and reconstruction algorithm based on PET detector model approximation. Our baseline single-threaded implementation provides reconstruction output image for 20 iterations within few minutes. Our future work is to optimize this implementation and to finally design 3D space reconstruction algorithm for final PET detector providing output in a reasonable time. This implies a need for heavy optimization and usage of modern computing techniques.

Acknowledgments: We acknowledge the technical and administrative support by M. Adamczyk, T. Gucwa-Ryś, A. Heczko, K. Łojek, M. Kajetanowicz, G. Konopka-Cupiał, J. Majewski, and W. Migdał and the financial support by the Polish National Center for Development and Research and by the Foundation for Polish Science through MPD program, the EU and MSHE Grant No. POIG.02.03.00-00-013/09.

Received October 29, 2013; accepted January 7, 2014

References

1. Shepp LA, Vardi Y. Maximum likelihood reconstruction in positron emission tomography. IEEE Trans Med Imaging 1982;MI-1:113–22.
2. Shepp LA, Vardi Y, Kaufman L. A statistical model for positron emission tomography. J Am Stat Assoc 1985;80:8–20.
3. Moskal P, Salabura P, Silarski M, Smyrski J, Zdebik J, Zieliński M. Novel detector systems for the positron emission tomography. Bio-Algorithms Med-Syst 2011;7:73.
4. Moskal P, Bednarski T, Białas P, Ciszewska M, Czerwiński E, Heczko A, et al. Strip-PET: a novel detector concept for the TOF-PET scanner. Nucl Med Rev C 2012;15:68–9.
5. Moskal P, Bednarski T, Białas P, Ciszewska M, Czerwiński E, Heczko A, et al. TOF-PET detector concept based on organic scintillators. Nucl Med Rev C 2012;15:81–4.
6. Parra L, Berret HH. List-mode likelihood EM algorithm and noise estimation demonstrated on 2D-PET. IEEE Trans Med Imaging 1998;17:228–35.
7. Berret HH, White T, Parra L. List-mode likelihood. J Opt Soc Am A Opt Image Sci Vis 1997;14:2914–23.